

# Inhibition of EGFR Signaling and Activation of Mitochondrial Apoptosis Contribute to Tanshinone IIA-Mediated Tumor Suppression in Non-Small Cell Lung Cancer Cells

This article was published in the following Dove Press journal:  
*OncoTargets and Therapy*

Feng Gao<sup>1,2,\*</sup>  
Ming Li<sup>1,3,4,\*</sup>  
Wenbin Liu<sup>5</sup>  
Wei Li<sup>2,6</sup>

<sup>1</sup>Cell Transplantation and Gene Therapy Institute, The Third Xiangya Hospital, Central South University, Changsha, Hunan 410013, People's Republic of China; <sup>2</sup>Department of Ultrasonography, The Third Xiangya Hospital of Central South University, Changsha, Hunan 410013, People's Republic of China; <sup>3</sup>School of Stomatology, Hunan University of Chinese Medicine, Changsha, Hunan 410208, People's Republic of China; <sup>4</sup>Changsha Stomatological Hospital, Hunan University of Chinese Medicine, Changsha, Hunan, 410004, People's Republic of China; <sup>5</sup>Department of Pathology, The Affiliated Hunan Cancer Hospital of Central South University, Changsha, Hunan 410013, People's Republic of China; <sup>6</sup>Department of Radiology, The Third Xiangya Hospital of Central South University, Changsha, Hunan 410013, People's Republic of China

\*These authors contributed equally to this work

**Background:** Deregulation of epidermal growth factor receptor (EGFR) signaling plays a critical role in non-small cell lung cancer (NSCLC) tumorigenesis. The natural product Tanshinone IIA (Tan IIA) exhibits significant anti-tumor effect in various human cancers, however, the mechanism remains elusive.

**Methods:** The inhibitory effect of Tan IIA NSCLC cells was determined by MTS and soft agar assays. The activation of EGFR signaling and the protein level of myeloid cell leukemia 1 (Mcl-1) were examined by immunoblot (IB), immunohistochemical staining (IHC), and ubiquitination analysis. The in vivo anti-tumor effect was validated by the xenograft mouse model.

**Results:** Tan IIA inhibits NSCLC cells through suppression of EGFR signaling. Tan IIA decreases cell viability and colony formation in EGFR wild type and activating mutant cell lines. The IB data further confirmed that Tan IIA suppresses EGFR phosphorylation time- and dose-dependently. Tan IIA destabilizes Mcl-1 and shortens the half-life. Ubiquitination analysis showed that treatment with Tan IIA promotes Mcl-1 ubiquitination and degradation. Further study showed that the downregulation of EGFR-Akt signaling is required for Tan IIA-induced Mcl-1 reduction. Ectopic overexpression of constitutively activated Akt1 compromised these antitumor efficacies in Tan IIA-treated NSCLC cells. Finally, Tan IIA inhibited the in vivo tumor growth.

**Conclusion:** Our data indicate that Tan IIA acts as an EGFR signaling inhibitor, and targeting EGFR-Akt-Mcl1 axis could provide a new option for NSCLC treatment.

**Keywords:** non-small cell lung cancer, Tanshinone IIA, epidermal growth factor receptor, Mcl-1, ubiquitination

## Introduction

Non-small cell lung cancer (NSCLC) is one of the leading causes of cancer-related death worldwide. Lung squamous cell carcinoma and adenocarcinoma are the most common subtypes of NSCLC. Early studies revealed that beyond tobacco smoking, the inherited genetic susceptibility is closely related to increased NSCLC risk.<sup>1</sup> The somatic mutations in the epidermal growth factor receptor (EGFR), Kirsten rat sarcoma (KRAS), and Phosphatidylinositol-4,5-Bisphosphate 3-Kinase catalytic subunit alpha (PIK3CA), and rearrangements of anaplastic lymphoma kinase (ALK) are frequently present in NSCLC, suggesting their critical roles in tumorigenesis and representing

Correspondence: Wei Li  
Tel +86 731-88618643  
Email weilix@csu.edu.cn

attractive targets for anti-cancer treatment.<sup>1–3</sup> Currently, the EGFR targeted therapies have become first-line therapeutic intervention for EGFR activating mutations harbored patients. Tyrosine kinase inhibitors (TKIs), including gefitinib, erlotinib, and osimertinib, have been developed to inhibit EGFR signaling specifically, promoted overall survival (OS) and longer progression-free survival (PFS) compared to that of conventional chemotherapy in advanced EGFR activating mutant NSCLC patients.<sup>3–6</sup> However, primary and acquired resistances are still the main reasons to cause TKIs treatment failure.<sup>6,7</sup> Thus, develop novel antitumor agents or identify new therapeutic targets will provide alternative strategies for NSCLC management.

The biological activities and chemical constituents of Danshen have been well studied over the past decades.<sup>8,9</sup> Tanshinone IIA (Tan IIA), one of the most abundant lipophilic components isolated from Danshen, exhibits significant antitumor efficacy in multiple human cancer types, including liver,<sup>10</sup> prostate,<sup>11</sup> breast,<sup>12</sup> colorectal,<sup>13</sup> and lung<sup>14</sup> cancer. The mechanism studies demonstrated that suppression of kinase activity and downregulation of the protein level of oncogenetic transcription factors were involved in the Tan IIA-mediated antitumor effect.<sup>15–19</sup> However, the function of Tan IIA on EGFR signaling and the mechanisms of how Tan IIA inhibits human NSCLC cancer cells remain undefined.

In this study, we found that Tan IIA exhibits a significant inhibitory effect on NSCLC cells by targeting EGFR-Mcl-1 signaling. We investigated the underlying mechanism using the *in vitro* and *in vivo* assays. Our data indicate that Tan IIA as a potential antitumor agent for NSCLC treatment.

## Materials and Methods

### Cell Culture and Antibodies

Human NSCLC cells, including HCC827, H1975, and A549, and the immortalized lung epithelial cells HBE and NL20, immortalized lung fibroblast cell MRC5, were obtained from American Type Culture Collection (ATCC, Manassas, VA). All cells were maintained at the incubator according to the standard protocols and subjected to routinely checking for mycoplasma contamination. Antibodies against p-EGFR (#3777), p-Akt (#4060), p-ERK1/2 (#4370), VDAC1 (#4866), cleaved-PARP (#5625), cleaved-caspase 3 (#9664), Mcl-1 (#94296), Bcl-xL (#2764), Bcl-2 (#4223), VDAC1 (#4661), Bax (#14796), Cytochrome c (#4280),  $\beta$ -actin (#3700), Akt (#2920), ubiquitin (#3936), and  $\alpha$ -Tubulin

(#2144) were purchased from Cell Signaling Technology, Inc. (Beverly, MA). The natural product Tanshinone IIA (>99%), PD98059, and LY294002 were purchased from Selleck Chemicals (Houston, TX). Lipofectamine 2000 transfection reagent (Thermo Fisher Scientific, Waltham, MA) was used for transient transfection following the manufacturer's instructions.

### MTS Assay

The CellTiter 96<sup>®</sup> Aqueous One Solution Cell Proliferation Assay kit (Promega, Madison, WI) was obtained from Promega (Madison, WI). The cells were seeded into 96-well plates at a density of  $2 \times 10^3$ /well and treated with Tanshinone IIA for various time points. Cell viability analysis was performed according to the standard protocol.

### Soft Agar Assay

The soft agar assay was performed as described previously.<sup>20</sup> Briefly, NSCLC cells were counted at a density of 8000 cells/mL and suspended in 1 mL of Eagle's basal medium containing 10% FBS, 0.3% agar, and Tanshinone IIA. The mixture was overlaid into 6-well plates with a 0.6% agar base. Cells were maintained in the incubator for 15 days, and the colony was counted with a microscope.

### Western Blot Analysis

The Western blot analysis was performed as described previously.<sup>21</sup> Briefly, The whole-cell extract (WCE) was prepared with the RIPA buffer and concentrated using the BCA protein assay (Thermo Fisher Scientific, Waltham, MA). For Western blot analysis, 20  $\mu$ g of WCE were subjected to SDS-PAGE electrophoresis. Proteins were then transferred to the PVDF membrane. After incubation with the primary antibody and second antibody sequentially, the protein was visualized by the ECL chemiluminescence (Thermo Fisher Scientific, Waltham, MA).

### Ubiquitination Analysis

The ubiquitination assay was performed as described previously.<sup>22</sup> Briefly, whole-cell lysates were prepared with modified RIPA buffer (1% SDS) supplemented with N-Ethylmaleimide (NEM) and protease inhibitors. The lysate was boiled at 95°C for 15 min and diluted with 0.1% SDS containing RIPA buffer. After centrifuge, the supernatant was incubated with Mcl-1 antibody together with protein A-Sepharose beads overnight at 4°C. The

beads were boiled with loading buffer and subjected to immunoblotting (IB) analysis.

## Isolation of Subcellular Fractions

The cytosolic and mitochondrial fractions were prepared using the Mitochondria Isolation Kit (Thermo Fisher Scientific, Waltham, MA) according to the manufacturers' instructions.

## In vivo Tumor Growth

The in vivo experiments were approved by the Animal Ethics Committee of Central South University. HCC827 ( $3 \times 10^6/100 \mu\text{L}$ ) cells in PBS were injected into the right flank of 6-week-old female athymic nude mice. Tanshinone IIA treatment at a dose of 10 mg/kg was initiated daily by i.p. injection when tumor volume reached  $100 \text{ mm}^3$ , whereas the control group was administered with vehicle control. Mouse body weight was recorded, and the tumor volume was measured with calipers every 2 days. Tumor volume was calculated following the formula of  $A \times B^2 \times 0.5$ . The A is the longest diameter of the tumor, B is the shortest diameter, and  $B^2$  is B squared.

## Immunohistochemical Staining

The immunohistochemical (IHC) staining was performed as described previously.<sup>23</sup> Briefly, the slide was deparaffinized for 1 h at  $60^\circ\text{C}$  and rehydrated in ddH<sub>2</sub>O. The antigen retrieval was performed by immersing into boiling sodium citrate buffer (10 mM, pH 6.0) for 10 min. After treated with 3% H<sub>2</sub>O<sub>2</sub> for 10 min, the slide was blocked with 50% goat serum albumin for 1 h at room temperature, followed by incubation with primary and second antibodies. The DAB Substrate Kit (Thermo Fisher Scientific) was used for visualization.

## Statistical Analysis

The Statistics Package for Social Science (SPSS) software (version 13.0; SPSS, Chicago, IL, USA) was used for Standard statistical analysis. The qualified data were presented as mean values  $\pm$  S.D. and analyzed using the Student's *t*-test or ANOVA. A *p*-value  $< 0.05$  was considered statistically significant.

## Results

### Tan IIA Inhibits NSCLC Cell Growth

Early studies indicated that Tan IIA (Figure 1A) exhibits a profound antitumor effect in various human cancer types.

However, the inhibitory effect of Tan IIA on NSCLC cells and the underlying mechanisms were not clear. In this study, we first examined the cytotoxic effect of Tan IIA on immortalized human lung epithelial and fibroblast cells. As shown in Figure 1B, Tan IIA had no significant inhibitory effect against HBE, NL20, and MRC5 cells at the concentrations  $\leq$  of  $20 \mu\text{M}$ . In contrast, the MTS results showed that Tan IIA suppressed cell viability of HCC827, H1975, and A549 cells dose- and time-dependently (Figure 1C). Treatment with Tan IIA at  $1 \mu\text{M}$  for 24 h attenuated cell viability in HCC827 and H1975 cells over 30%, and this inhibitory efficacy was reached over 50% after treatment with Tan IIA for 72 h. Furthermore, exposure to a higher concentration of Tan IIA ( $5 \mu\text{M}$ ) exhibited a much stronger inhibitory effect of cell viability when compared to that of 1 or  $2 \mu\text{M}$  Tan IIA treatment (Figure 1C). We next determined the effects of Tan IIA on colony formation of these NSCLC cells. The results indicated that Tan IIA reduced the anchorage-independent growth of HCC827, H1975, and A549 cells significantly. The colony number, as well as the colony size, was reduced in a dose-dependent manner (Figure 1D). Furthermore, treatment with  $5 \mu\text{M}$  Tan IIA blocked colony formation in these tested cancer cells (Figure 1D). These results suggest that Tan IIA has no obvious cytotoxic effect on immortalized lung cells, but inhibits NSCLC cells significantly.

### Tan IIA Suppresses EGFR Signaling

Because the EGFR kinase plays a crucial role in lung tumorigenesis, we determined the effect of Tan IIA on EGFR signaling. The HCC827, H1975, and A549 cells, which harbor the EGFR Exon 19 deletion mutation, L858R/T790M mutation, and WT EGFR, were chosen for further study. The results showed that Tan IIA inhibited EGFR phosphorylation dose-dependently (Figure 2A) in HCC827, H1975, and A549 cells. Moreover, the activation of downstream target kinases, Akt, and ERK1/2, was decreased robustly (Figure 2A), suggesting that Tan IIA could suppress the activity of both activating mutant and WT EGFRs. We next examined the effect of Tan IIA on EGF-induced EGFR activation. As shown in Figure 2B, Tan IIA substantially inhibited EGF-induced EGFR, Akt, and ERK1/2 phosphorylation (Figure 2B). Moreover, pretreated with Tan IIA reduced EGF-induced EGFR activation at various time points (Figure 2C) in HCC827 cells. These results indicate that Tan IIA inhibits EGFR signaling in NSCLC cells dose-dependently.

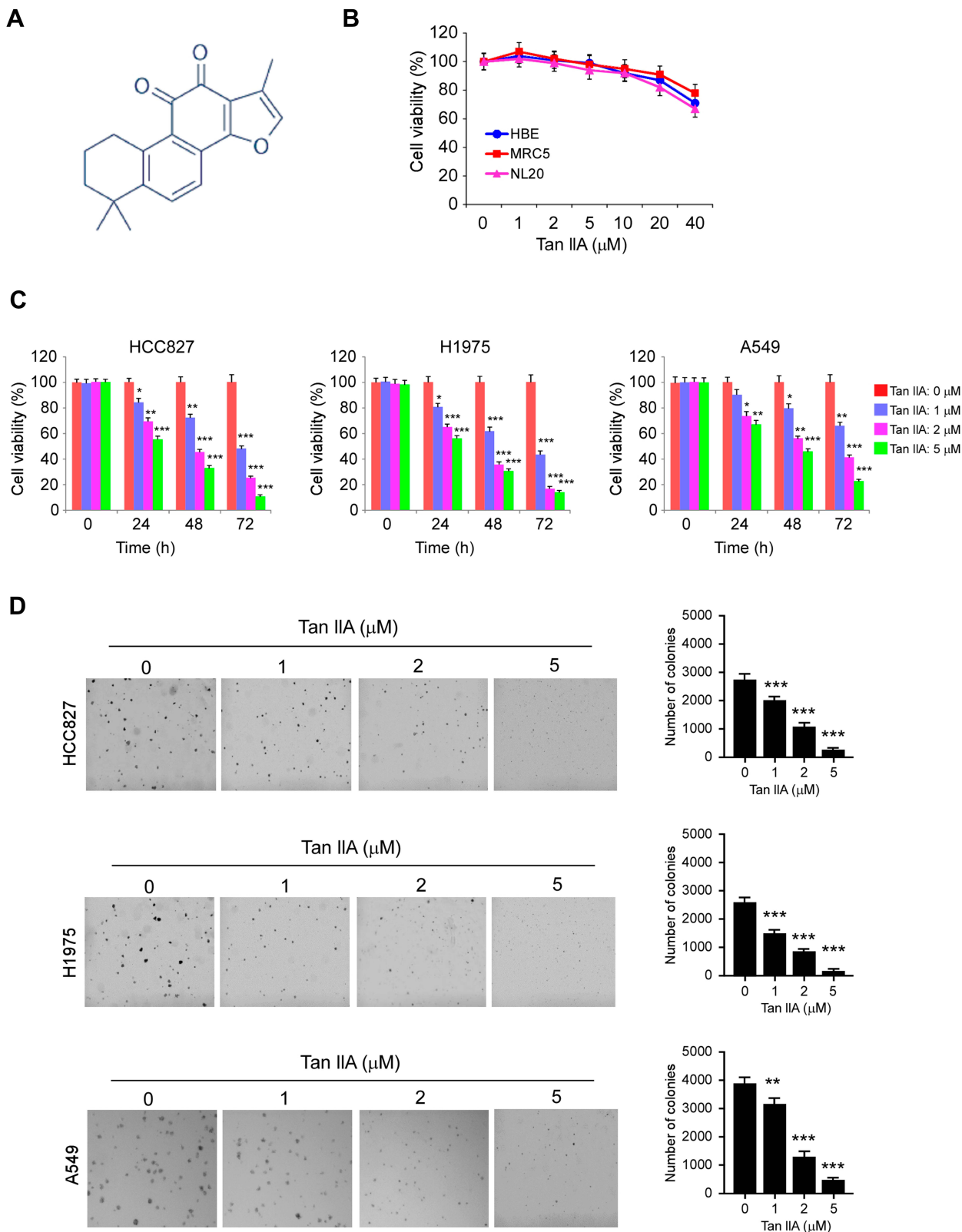


**Figure 1** The effects of Tanshinone IIA (Tan IIA) on NSCLC and immortalized lung cells. **(A)** the chemical structure of Tan IIA. **(B)** Cytotoxicity of Tan IIA on immortalized HBE, MRC5, and NL20 cells. The cells were treated with Tan IIA for 24 h. Cell viability was measured by MTS assay. **(C)** MTS assay analyzes the effect of Tan IIA on cell viability of HCC827 (left), H1975 (middle), and A549 (right) cells. **(D)** Soft agar assay analyzes the effect of Tan IIA on colony formation of HCC827 (top), H1975 (middle), and A549 (bottom) cells. \* $p < 0.01$ , \*\* $p < 0.01$ , \*\*\* $p < 0.001$ .

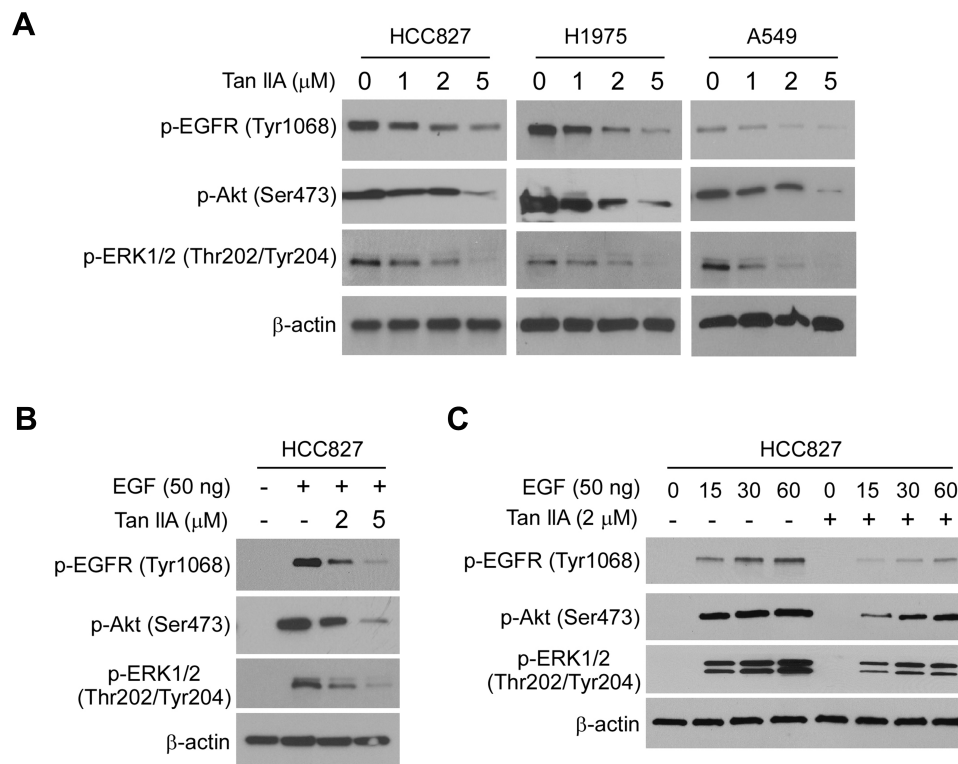


**Figure 2** Tan IIA inhibits EGFR signaling. **(A)** Tan IIA suppresses EGFR signaling in NSCLC cells. Whole-cell extract (WCE) from Tan IIA-treated HCC827 (left), H1975 (middle), and A549 (right) were subjected to immunoblotting (IB) analysis. **(B)** Tan IIA inhibits EGF-induced EGFR activation. HCC827 cells were starved overnight, and pre-treated with Tan IIA for 2 h. The cells were stimulated with EGF for 30 min, WCE was subjected to IB analysis. **(C)** Tan IIA down-regulates EGF-induced EGFR activation. HCC827 cells were starved overnight, and pre-treated with Tan IIA for 2 h. The cells were treated with EGF, and WCE was collected with various time points and subjected to IB analysis.

## Tan IIA Promotes the Intrinsic Apoptosis Pathway

To determine whether Tan IIA inhibited EGFR signaling could cause cell death, we pre-treated NSCLC cells with various inhibitors. The results showed that the apoptosis inhibitor z-VAD-fmk, but not the necroptosis inhibitor Necrostatin-1, or the autophagy inhibitor 3-MA, significantly rescued Tan IIA-induced cell viability suppression in HCC827, H1975, and A549 cells (Figure 3A). Moreover, the trypan blue exclusion assay showed that z-VAD-fmk increased the population of live cells after Tan IIA treatment (Figure 3B). To confirm that Tan IIA promoted apoptosis, we examined the expression of cleaved-PARP and -caspase 3. As shown in Figure 3C, Tan IIA increased the protein level of cleaved-PARP and -caspase 3 dose-dependently. Moreover, the enzyme activity of caspase 3 was enhanced in the presence of Tan IIA (Figure 3D). The flow cytometry data also showed that Tan IIA increased the apoptosis cells in a dose-dependent manner (Figure 3E). We next isolated the subcellular fractions of Tan IIA-treated HCC827 cells. The results showed that Tan IIA promoted the release of cytochrome C from mitochondria to the cytoplasm.

Consistently, the protein level of Bax in cytosolic fraction was decreased dose-dependently (Figure 3F), indicating Tan IIA activates the mitochondrial apoptosis signaling. Because down-regulation of the pro-survival Bcl-2 family membranes was often observed in intrinsic apoptosis signaling activated cells, we examined the expression of Bcl-2, Bcl-xL, and Mcl-1 in Tan IIA-treated HCC827 cells. The results showed that the expression of Mcl-1, but not Bcl-2 or Bcl-xL, decreased substantially after Tan IIA treatment (Figure 3G). These results suggest that Tan IIA induces apoptosis in NSCLC cells.

## Tan IIA Induces Ubiquitination-Mediated Mcl-1 Degradation

To determine the mechanism of how Tan IIA decreased Mcl-1 protein level, we treated NSCLC cells with the proteasome inhibitor, MG132. Our results showed that Tan IIA-induced reduction of Mcl-1 was compromised in the presence of MG132 (Figure 4A). Furthermore, the mRNA level determined by qRT-PCR revealed that Tan IIA did not decrease the transcription of Mcl-1 in these NSCLC cells (Figure 4B). To further validate that Tan IIA promoted Mcl-1 degradation,

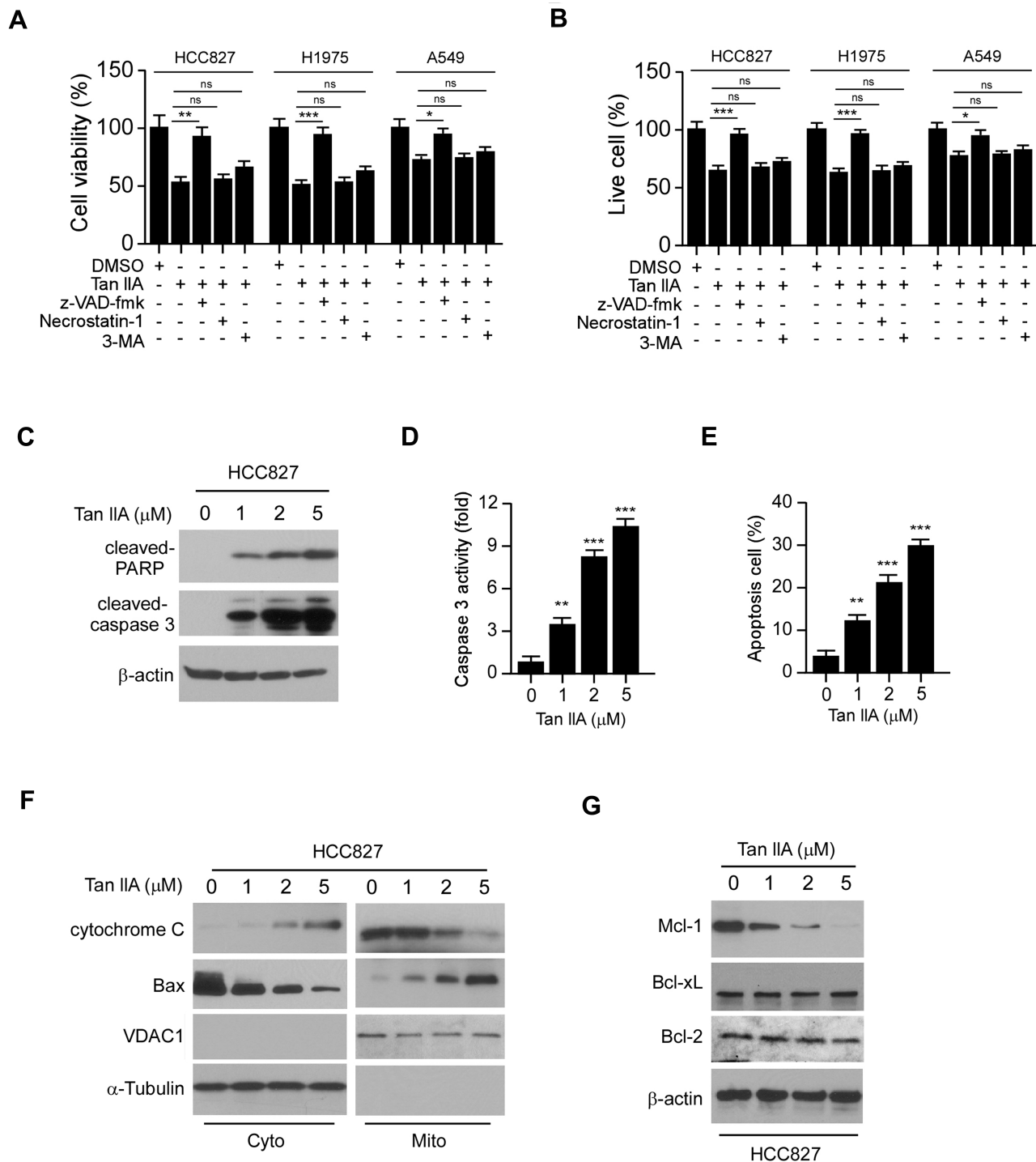


**Figure 3** Tan IIA induces apoptosis in NSCLC cells. **(A)** MTS assay analyzes the cell viability of NSCLC cells treated with multiple small molecular inhibitors and Tan IIA. **(B)** trypan blue exclusion assay analyzes live cell population of NSCLC cells treated with multiple small molecular inhibitors and Tan IIA. **(C)** HCC827 cells were treated with Tan IIA, WCE was subjected to IB analysis. **(D)** HCC827 cells were treated with Tan IIA and subjected to caspase 3 activity analysis. **(E)** Flow cytometry analyzes apoptosis of HCC827 cells treated with Tan IIA. **(F)** HCC827 cells were treated with Tan IIA, the subcellular fractions were isolated and subjected to IB analysis. **(G)** HCC827 cells were treated with Tan IIA, WCE was subjected to IB analysis. \* $p < 0.01$ , \*\* $p < 0.01$ , \*\*\* $p < 0.001$ .

we performed the CHX assay to examine the half-life of Mcl-1 protein. As shown in Figure 4C, the half-life of Mcl-1 was decreased from around 3.5 h to 1.5 h after Tan IIA treatment, indicating that Tan IIA promoted the instability of Mcl-1. We

next determined whether Tan IIA induced Mcl-1 ubiquitination in NSCLC cells. As shown in Figure 4D, treatment with Tan IIA enhanced the endogenous Mcl-1 ubiquitination in HCC827 cells. An early study showed that the ubiquitination

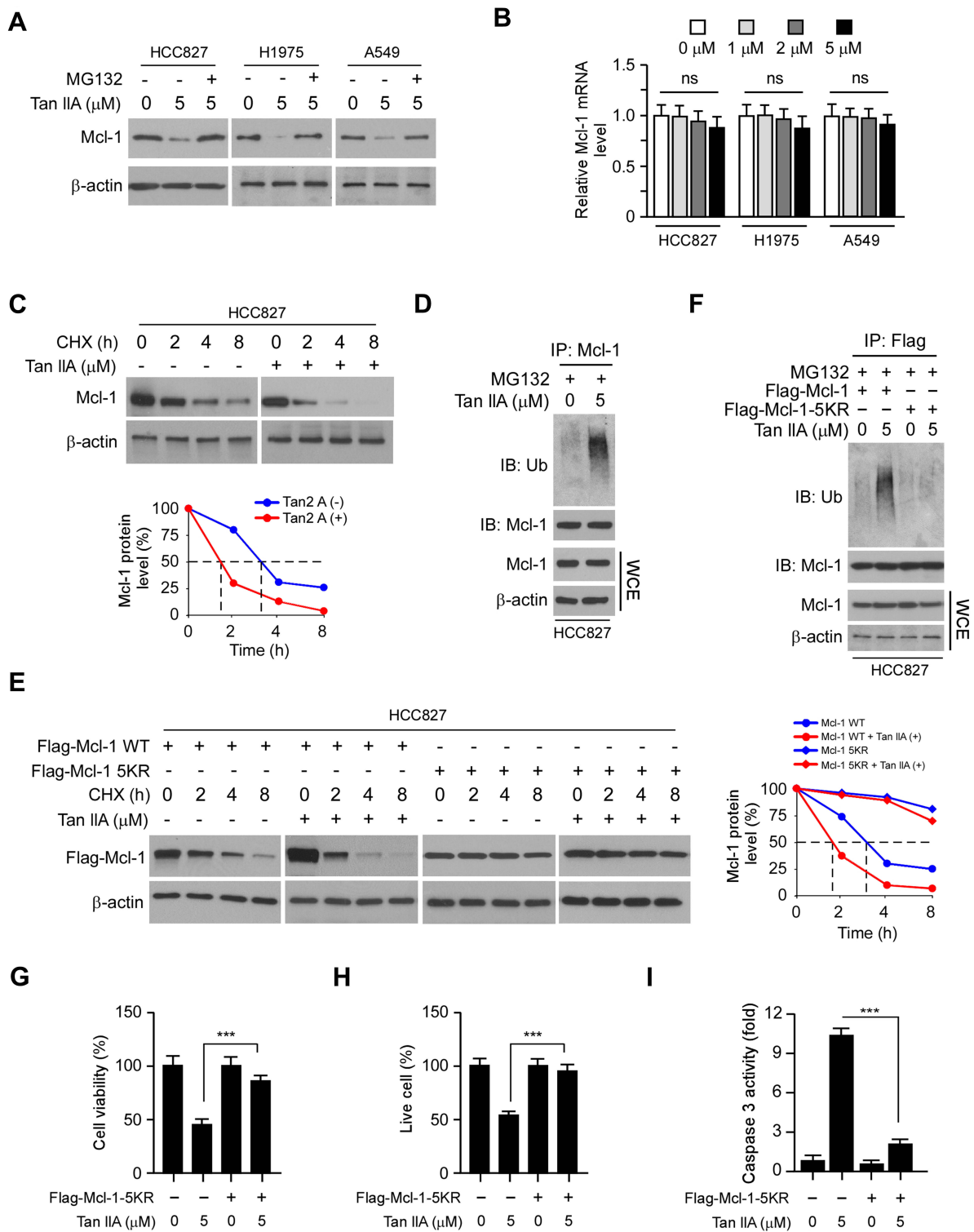


**Figure 4** Tan IIA promotes Mcl-1 degradation. **(A)** NSCLC cells were treated with Tan IIA for 24 h, followed by treated with MG132 for another 6 h. WCE was subjected to IB analysis. **(B)** qRT-PCR analyzes the mRNA levels of Mcl-1 in Tan IIA-treated NSCLC cells. **(C)** IB analyzes the half-life of Mcl-1 in Tan IIA-treated HCC827 cells. HCC827 cells were treated with Tan IIA for 24 h, followed by incubation with CHX for various time points. WCE was subjected to IB analysis. **(D)** Tan IIA promotes Mcl-1 ubiquitination. HCC827 cells were treated with Tan IIA for 24 h, followed by MG132 treatment for 6 h. WCE was collected and immunoprecipitated with Mcl-1 antibody plus agarose A/G beads overnight. Mcl-1 ubiquitination was examined by IB analysis. **(E)** IB analyzes the half-life of Mcl-1 WT and 5KR mutant in Tan IIA-treated HCC827 cells. HCC827 cells were transfected with Flag-Mcl-1 WT or Flag-Mcl-1 5KR for 24 h. The cells were then treated with Tan IIA for another 24 h and incubated with CHX for various time points. WCE was subjected to IB analysis. **(F)** IB analyzes the ubiquitination of Mcl-1 WT and 5KR. HCC827 cells were transfected with Flag-Mcl-1 WT or Flag-Mcl-1 5KR, followed by Tan IIA treatment for 24 h. WCE was collected and subjected to immunoprecipitation with Flag antibody and IB analysis. **(G and H)** MTS assay **(G)** and trypan blue exclusion assay **(H)** analysis of cell viability and live-cell population in Tan IIA-treated NSCLC cells with/without Mcl-1 5KR overexpression. **(I)** Caspase 3 activity of Tan IIA-treated NSCLC cells with/without Mcl-1 5KR overexpression. \*\*\* $p < 0.001$ .

of the 5 lysine residues, including K5, K40, K136, K194, and K197, was required for FBW7-mediated Mcl-1 degradation.<sup>24</sup> We thus generated a 5KR mutant, which contains the lysine to arginine mutation of these five lysine residues. The CHX assay showed that 5KR mutation prolonged the half-life of Mcl-1 protein from around 3.5 h to over 8 h (Figure 4E). Moreover, this 5KR mutation rescued Tan IIA-mediated shortened of Mcl-1 half-life and enhanced the protein stability robustly (Figure 4E). The ubiquitination assay revealed that Tan IIA promoted the ubiquitination of WT Mcl-1, but not that of the 5KR mutant (Figure 4F). Furthermore, overexpression of Mcl-1-5KR significantly decreased Tan IIA induced-apoptosis, as the cell viability and the population of live cells were increased in Mcl-1-5KR overexpressed HCC827 cells when compared to that of Tan IIA-treated control cells (Figure 4G and H). In addition, the activity of cleaved-caspase3 was reduced consistently (Figure 4I). These results suggest that Tan IIA promotes Mcl-1 degradation in an ubiquitination-dependent manner.

## Overexpression of Myr-Akt1 Rescues Tan IIA-Induced Mcl-1 Degradation and Apoptosis

We next determined whether the destruction of Mcl-1 is required for Tan IIA-induced apoptosis in NSCLC cells. As shown in Figure 5A, overexpression of Mcl-1 attenuated Tan IIA-enhanced the expression of cleaved-PARP and-caspase 3. Consistently, the MTS assay and trypan blue exclusion assay showed that ectopic overexpression of Mcl-1 rescued the reduction of cell viability (Figure 5B), and increased the population of live cells (Figure 5C) in Tan IIA-treated NSCLC cells. Furthermore, the activity of caspase 3 was decreased significantly in Mcl-1 overexpressed HCC827 cells with Tan IIA treatment (Figure 5D). These results imply that the decrease of Mcl-1 contributes to Tan IIA-induced apoptosis. We next investigated which signaling pathway was involved in Mcl-1 degradation. Because treated with Tan IIA caused a striking inhibitory effect on EGFR signaling, we pre-treated HCC827 cells with the small molecular inhibitors to block the activation of EGFR downstream kinases Akt and ERK1/2. As shown in Figure 5E, the Akt signaling inhibitor LY294002, but not the ERK1/2 inhibitor PD98059, inhibited Mcl-1 expression in HCC827 cells. Consistently, overexpression of constitutively activated Akt, Myr-Akt1, up-regulated Mcl-1 protein level in Tan IIA untreated cells, and rescued Mcl-1 expression in Tan IIA-treated cells (Figure 5F). In addition, the expression of apoptosis markers, cleaved-caspase 3 and -PARP, were reduced

robustly in Myr-Akt1 transfected HCC827 cells (Figure 5F). The results from MTS assay, trypan blue exclusion assay, and measurement of caspase 3 activation, further confirmed that ectopic overexpression of Myr-Akt1 compromised Tan IIA-induced apoptosis in HCC827 cells (Figure 5G–I). Also, Tan IIA-induced activation of mitochondria apoptosis was impaired with Myr-Akt1 transfection, as the release of cytochrome C from mitochondria to the cytoplasm, and the expression of Bax on mitochondria were reduced (Figure 5J). Our data indicate that inhibits of EGFR-Akt signaling is associated with Tan IIA-induced Mcl-1 degradation and apoptosis induction.

## Tan IIA Suppresses in vivo Tumor Growth

We next determined the in vivo antitumor effects of Tan IIA using a xenograft mouse model. The results revealed that the average tumor volume of the vehicle-treated HCC827-derived xenograft tumor was  $625 \pm 111$  mm<sup>3</sup>. In contrast, treatment with Tan IIA delayed in vivo tumor development significantly, as the average tumor volume was  $281 \pm 56$  mm<sup>3</sup> (Figure 6A). Furthermore, the size of the tumor mass from the Tan IIA-treated group was smaller than that of the vehicle-treated group (Figure 6B). The average tumor weight of the vehicle-treated group was significantly heavier than that of Tan IIA administrated tumors (Figure 6C). In addition, treatment with Tan IIA for two weeks did not cause the loss of body weight significantly (Figure 6D). Immunohistochemical staining analysis was performed to examine the in vivo inhibitory effect of Tan IIA on EGFR activation. As shown in Figure 6E and F, the positive staining of EGFR phosphorylation was suppressed in Tan IIA-treated tumors. Consistently, the population of ki67 positive cells was reduced, indicating that Tan IIA inhibited cell proliferation in vivo. These results confirm the in vivo antitumor effects of Tan IIA in an NSCLC xenograft model.

## Discussion

Over the past several decades, NSCLC has been one of the most common cancers and cancer-related death in the world. Each year, over one million new cases of NSCLC are diagnosed. However, only 25% is suitable for surgical treatment. The 5-year overall survival (OS) rate for patients with metastatic NSCLC was less than 5%.<sup>25,26</sup> Currently, the systemic therapeutic strategy for advanced NSCLC is determined based on the presence of genetic biomarkers. The alteration of oncogenes, including activating mutation of EGFR, rearrangements of ALK and ROS1,



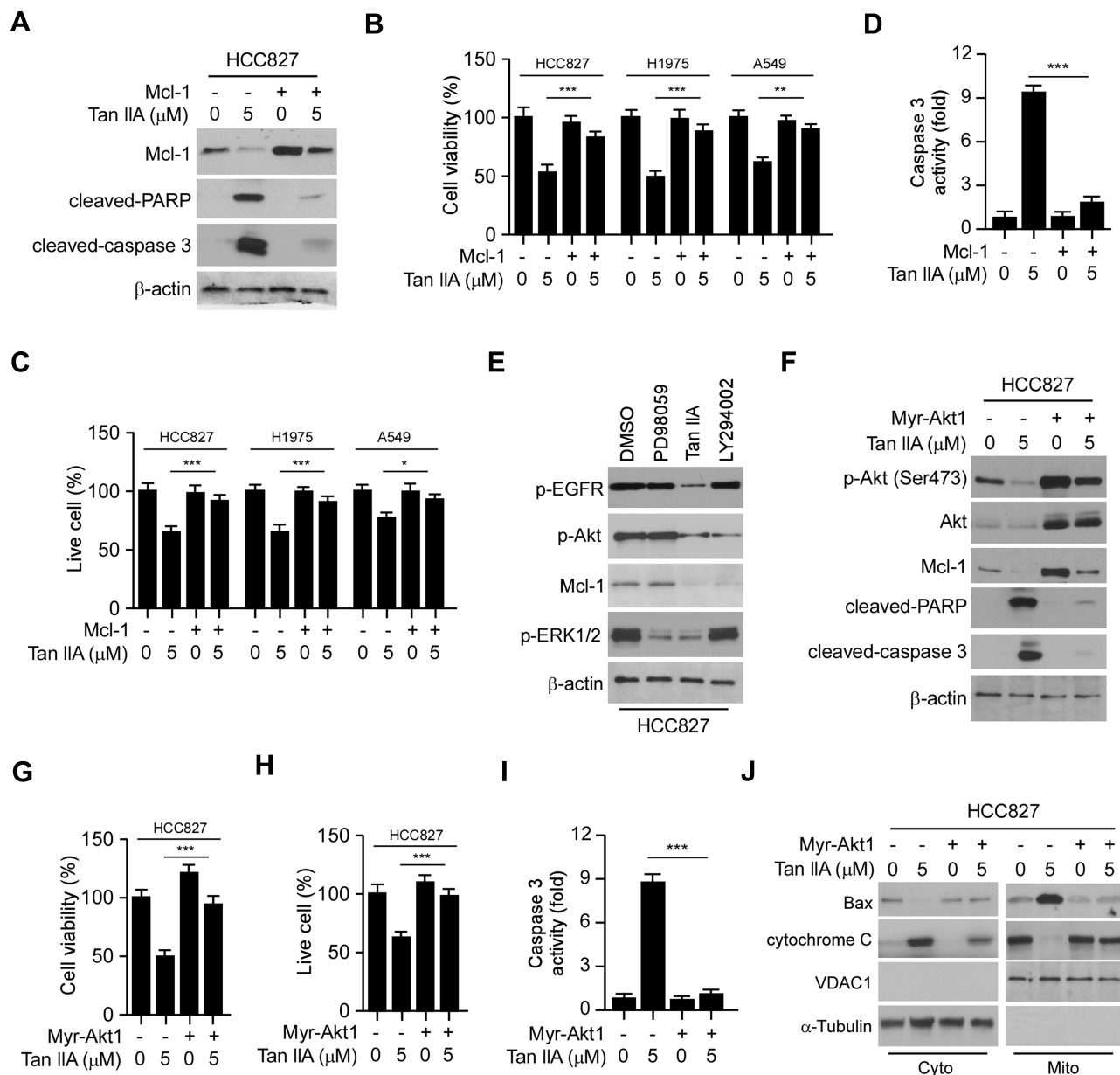


**Figure 5** Overexpression of Myr-Akt1 restored Mcl-1 expression and rescued apoptosis in NSCLC cells. **(A)** HCC827 cells were transfected with Mcl-1 construct and treated with Tan IIA, WCE was subjected to IB analysis. **(B and C)** MTS assay **(B)** and trypan blue exclusion assay **(C)** analysis of cell viability and live-cell population in Tan IIA-treated NSCLC cells with Mcl-1 overexpression. **(D)** The enzyme activity of caspase 3 in Tan IIA-treated HCC827 cells with Mcl-1 overexpression. **(E)** HCC827 cells were treated with Tan IIA, PD98059, or LY294002, WCE was subjected to IB analysis. **(F)** IB analysis of apoptosis in Tan IIA-treated HCC827 cells with Myr-Akt1 transfection. **(G–I)** MTS assay **(G)**, trypan blue exclusion assay **(H)**, and caspase 3 activity analysis **(I)** were performed in Tan IIA-treated HCC827 cells with Myr-Akt1 overexpression. **(J)** HCC827 cells were transfected with Myr-Akt1 and treated with Tan IIA for 24 h. The subcellular fractions were isolated and subjected to IB analysis. \* $p < 0.01$ , \*\* $p < 0.01$ , \*\*\* $p < 0.001$ .

and V600E mutation of BRAF, are considered as a driving force for NSCLC tumorigenesis Targeted therapy for these driver mutations improves the progression-free survival (PFS) significantly compared to the traditional chemo/radiotherapy.<sup>1,27-29</sup> In the present study, we demonstrated that Tan IIA inhibits NSCLC through suppression of EGFR signaling. Tan IIA reduces the phosphorylation of both wild type (A549) and activating mutant (HCC827 and

H1975) EGFR in NSCLC cells. Furthermore, the activity of EGFR downstream kinases, Akt, and ERK1/2, is decreased with Tan IIA treatment. These results indicate that Tan IIA is a potential EGFR signaling inhibitor.

As one of the major biologically active constituents in Danshen, Tan IIA has been successfully used for coronary heart diseases, cerebrovascular diseases, and myocardial infarction treatment in the clinic.<sup>9,30,31</sup> In the past decades,

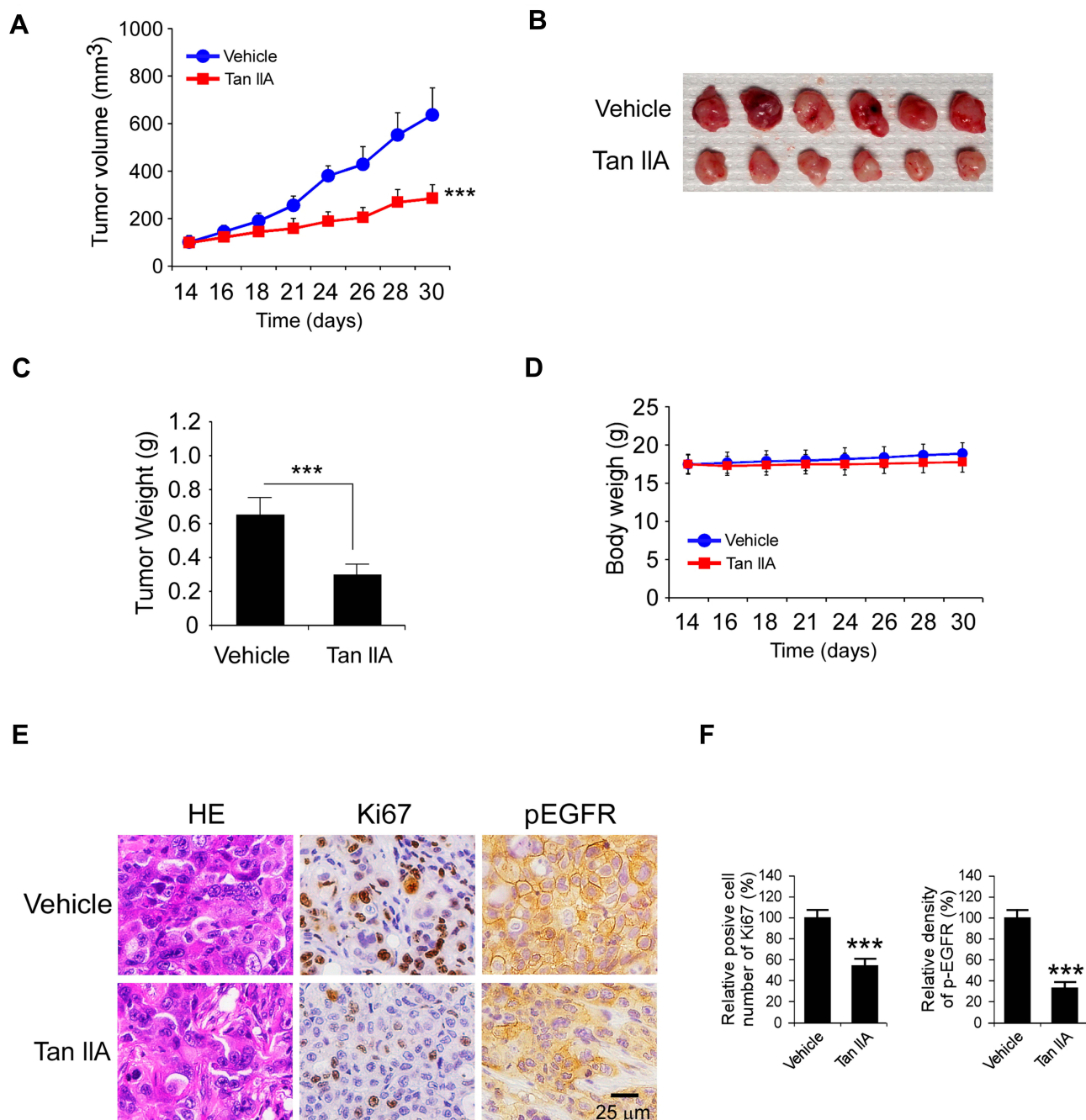


**Figure 6** Tan IIA inhibits in vivo tumor growth. **(A)** The tumor volumes of HCC827-derived xenograft tumors with vehicle or Tan IIA treatment. **(B and C)** The image of tumor mass **(B)** and tumor weight **(C)** of vehicle- or Tan IIA-treated xenograft tumors. **(D)** The body weight of tumor-bearing mouse with vehicle or Tan IIA treatment. **(E)** Immunohistochemical staining analysis of ki67 and p-EGFR in vehicle- or Tan IIA-treated xenograft tumors. **(F)** Qualification of ki67 and p-EGFR staining from **(E)**. \*\*\* $p < 0.001$ .

Tan IIA has attracted great interest in cancer prevention and chemotherapy due to its significant antitumor efficacy and minimal side effects. Recent reports revealed that Tan IIA inhibits NSCLC cells via down-regulating the PI3K/Akt signalling<sup>32</sup> and activating the JNK pathway.<sup>33</sup> Although the induction of mitochondrial apoptosis is involved in Tan IIA-mediated antitumor activity, the molecular mechanism

was not clear. Our data showed that Tan IIA promotes apoptosis, but not necroptosis in NSCLC cells. The IB data revealed that Tan IIA decreased the protein level of pro-survival Bcl-2 family member, Mcl-1, through inhibition of the EGFR-Akt axis. Overexpression of constitutively activated Akt1 compromised the antitumor efficacy of Tan IIA and reduced Tan IIA-induced mitochondrial apoptosis in

NSCLC cells. Moreover, ectopic overexpression of Mcl-1 attenuated Tan IIA-induced downregulation of cell viability and apoptosis, further confirmed that the reduction of Mcl-1 protein level is required for apoptosis induction with Tan IIA treatment. Importantly, recent studies reported that degradation of Mcl-1 is required for EGFR-TKIs-induced apoptosis in cancer cells. For example, decrease of Mcl-1 protein overcomes TKI acquired resistance in EGFR activating mutant NSCLC cells.<sup>34,35</sup> TKI treatment-induced Mcl-1 downregulation sensitizes cancer cells to Bcl-XL/Bcl2 inhibitor.<sup>36</sup> Furthermore, suppression of EGFR activity by erlotinib impaired the binding between Mcl-1 and Bim, which enhances the antitumor efficacy of ABT-737.<sup>37</sup> Our study revealed that Mcl-1 is a downstream target of EGFR-Akt signaling, and reduction of the Mcl-1 protein level might enhance the tumor-killing effect of EGFR inhibitors.

As a short half-life protein, the abundance of Mcl-1 is tightly regulated in multiple levels, including transcriptional, transcriptional, and posttranslational processes. The balance between ubiquitination and deubiquitination determines the turnover of Mcl-1 in human cancer cells. So far, multiple E3 ligases targeting Mcl-1 for degradation have been identified, such as FBW7<sup>38</sup> and  $\beta$ -Trcp.<sup>39</sup> In contrast, the deubiquitinases, including USP9X<sup>40</sup> and USP13,<sup>41</sup> which can specifically remove the K48-linked polyubiquitination chains reverse this ubiquitination process and is required for Mcl-1 stability. The previous study revealed that the 5 lysine (K) residues, including K5, K40, K136, K194, and K197, are potential ubiquitination sites that catalyzed by E3 ligase FBW7.<sup>24</sup> In this study, our results showed that Tan IIA shortens Mcl-1 half-life and promotes its ubiquitination. Treatment with the proteasome inhibitor MG132 rescues the Mcl-1 protein level. Moreover, mutation of the ubiquitination lysine sites robustly decreases Tan IIA-induced Mcl-1 ubiquitination. These results revealed a novel antitumor mechanism of Tan IIA and suggested that targeting protein degradation is a promising strategy for cancer treatment.

Overall, the present study identified that Tan IIA acts as an EGFR-Akt signaling inhibitor, and decrease of Mcl-1 protein level by ubiquitination is required for Tan IIA-mediated antitumor activity. Our data extend the antitumor mechanisms of Tan IIA, and targeting EGFR-Akt-Mcl-1 signaling is a promising approach for NSCLC treatment.

## Abbreviations

NSCLC, non-small cell lung cancer; Mcl-1, myeloid cell leukemia 1; IB, immunoblot; EGFR, epidermal growth

factor receptor; KRAS, Kirsten rat sarcoma; PIK3CA, Phosphatidylinositol-4,5-Bisphosphate 3-Kinase catalytic subunit alpha; ALK, anaplastic lymphoma kinase; TKIs, Tyrosine kinase inhibitors; PFS, progression-free survival; OS, overall survival; WCE, whole-cell extract; IHC, immunohistochemical; SD, standard deviation; PDB, Protein Data Bank1; AML, Acute Myelocytic Leukemia.

## Ethics and Consent Statement

The use and care of experimental animals were approved by the Institutional Animal Care and Use Committee of Central South University (2018-S116) according to the Guide for the Care and Use of Laboratory Animals (National Academies Press, Washington, DC).

## Funding

This work was supported by the National Natural Science Foundation of China (No.81904262, and No.81972837), the Natural Science Foundation of Hunan Province (2018JJ3787, 2018JJ2604, 2019JJ50682).

## Disclosure

The authors report no conflicts of interest in this work.

## References

- Herbst RS, Morgensztern D, Boshoff C. The biology and management of non-small cell lung cancer. *Nature*. 2018;553(7689):446–454. doi:10.1038/nature25183
- Skoulidis F, Heymach JV. Co-occurring genomic alterations in non-small-cell lung cancer biology and therapy. *Nat Rev Cancer*. 2019;19(9):495–509. doi:10.1038/s41568-019-0179-8
- Arbour KC, Riely GJ. Systemic therapy for locally advanced and metastatic non-small cell lung cancer: a review. *JAMA*. 2019;322(8):764–774. doi:10.1001/jama.2019.11058
- Leonetti A, Sharma S, Minari R, Perego P, Giovannetti E, Tiseo M. Resistance mechanisms to osimertinib in EGFR-mutated non-small cell lung cancer. *Br J Cancer*. 2019;121(9):725–737. doi:10.1038/s41416-019-0573-8
- Santoni-Rugiu E, Melchior LC, Urbanska EM, et al. Intrinsic resistance to EGFR-Tyrosine kinase inhibitors in EGFR-mutant non-small cell lung cancer: differences and similarities with acquired resistance. *Cancers (Basel)*. 2019;11(7):923. doi:10.3390/cancers11070923
- Wu SG, Shih JY. Management of acquired resistance to EGFR TKI-targeted therapy in advanced non-small cell lung cancer. *Mol Cancer*. 2018;17(1):38. doi:10.1186/s12943-018-0777-1
- Lim SM, Syn NL, Cho BC, Soo RA. Acquired resistance to EGFR targeted therapy in non-small cell lung cancer: mechanisms and therapeutic strategies. *Cancer Treat Rev*. 2018;65:1–10. doi:10.1016/j.ctrv.2018.02.006
- Zhang Y, Jiang P, Ye M, Kim SH, Jiang C, Lu J. Tanshinones: sources, pharmacokinetics and anti-cancer activities. *Int J Mol Sci*. 2012;13(10):13621–13666. doi:10.3390/ijms131013621
- Chen Z, Xu H. Anti-inflammatory and immunomodulatory mechanism of tanshinone IIA for atherosclerosis. *Evid Based Complement Alternat Med*. 2014;2014:267976. doi:10.1155/2014/267976

10. Ma L, Jiang H, Xu X, et al. Tanshinone IIA mediates SMAD7-YAP interaction to inhibit liver cancer growth by inactivating the transforming growth factor beta signaling pathway. *Aging (Albany NY)*. 2019;11(21):9719–9737. doi:10.18632/aging.v11i21
11. Wang M, Zeng X, Li S, et al. A novel tanshinone analog exerts anti-cancer effects in prostate cancer by inducing cell apoptosis, arresting cell cycle at G2 Phase and blocking metastatic ability. *Int J Mol Sci*. 2019;20(18):4459.
12. Li K, Liu W, Zhao Q, et al. Combination of tanshinone IIA and doxorubicin possesses synergism and attenuation effects on doxorubicin in the treatment of breast cancer. *Phytother Res*. 2019;33(6):1658–1669. doi:10.1002/ptr.v33.6
13. Xue J, Jin X, Wan X, et al. Effects and MECHANISM OF TANSHINONE II a in proliferation, apoptosis, and migration of human colon cancer cells. *Med Sci Monit*. 2019;25:4793–4800. doi:10.12659/MSM.914446
14. Wang R, Luo Z, Zhang H, Wang T. Tanshinone IIA reverses gefitinib-resistance in human non-small-cell lung cancer via regulation of VEGFR/Akt pathway. *Onco Targets Ther*. 2019;12:9355–9365. doi:10.2147/OTT.S221228
15. Luo H, Vong CT, Chen H, et al. Naturally occurring anti-cancer compounds: shining from Chinese herbal medicine. *Chin Med*. 2019;14:48.
16. Xu S, Liu P. Tanshinone II-A: new perspectives for old remedies. *Expert Opin Ther Pat*. 2013;23(2):149–153. doi:10.1517/13543776.2013.743995
17. Bai Y, Zhang L, Fang X, Yang Y. Tanshinone IIA enhances chemosensitivity of colon cancer cells by suppressing nuclear factor-kappaB. *Exp Ther Med*. 2016;11(3):1085–1089. doi:10.3892/etm.2016.2984
18. Lv C, Zeng HW, Wang JX, et al. The antitumor natural product tanshinone IIA inhibits protein kinase C and acts synergistically with 17-AAG. *Cell Death Dis*. 2018;9(2):165. doi:10.1038/s41419-017-0247-5
19. Guo Y, Li Y, Wang FF, et al. The combination of Nutlin-3 and Tanshinone IIA promotes synergistic cytotoxicity in acute leukemic cells expressing wild-type p53 by co-regulating MDM2-P53 and the AKT/mTOR pathway. *Int J Biochem Cell Biol*. 2019;106:8–20. doi:10.1016/j.biocel.2018.10.008
20. Zhou L, Yu X, Li M, et al. Cdhl-mediated Skp2 degradation by dioscin reprogrammes aerobic glycolysis and inhibits colorectal cancer cells growth. *EBioMedicine*. 2019;51:102570.
21. Liu W, Li W, Liu H, Yu X. Xanthohumol inhibits colorectal cancer cells via downregulation of Hexokinases II-mediated glycolysis. *Int J Biol Sci*. 2019;15(11):2497–2508. doi:10.7150/ijbs.37481
22. Yu X, Wang R, Zhang Y, et al. Skp2-mediated ubiquitination and mitochondrial localization of Akt drive tumor growth and chemoresistance to cisplatin. *Oncogene*. 2019;38(50):7457–7472. doi:10.1038/s41388-019-0955-7
23. Liu H, Li W, Yu X, et al. EZH2-mediated Puma gene repression regulates non-small cell lung cancer cell proliferation and cisplatin-induced apoptosis. *Oncotarget*. 2016;7(35):56338–56354. doi:10.18632/oncotarget.10841
24. Inuzuka H, Shaik S, Onoyama I, et al. SCF(FBW7) regulates cellular apoptosis by targeting MCL1 for ubiquitylation and destruction. *Nature*. 2011;471(7336):104–109. doi:10.1038/nature09732
25. Tucker WS, Kirsch WM, Martinez-Hernandez A, Fink LM. In vitro plasminogen activator activity in human brain tumors. *Cancer Res*. 1978;38(2):297–302.
26. De Ruyscher D, Faivre-Finn C, Nackaerts K, et al. Recommendation for supportive care in patients receiving concurrent chemotherapy and radiotherapy for lung cancer. *Ann Oncol*. 2020;31(1):41–49. doi:10.1016/j.annonc.2019.10.003
27. Guo Y, Cao R, Zhang X, et al. Recent progress in rare oncogenic drivers and targeted therapy for non-small cell lung cancer. *Onco Targets Ther*. 2019;12:10343–10360. doi:10.2147/OTT.S230309
28. Yuan M, Huang LL, Chen JH, Wu J, Xu Q. The emerging treatment landscape of targeted therapy in non-small-cell lung cancer. *Signal Transduct Target Ther*. 2019;4:61. doi:10.1038/s41392-019-0099-9
29. Gao J, HR L, Jin C, Jiang JH, Ding JY. Strategies to overcome acquired resistance to EGFR TKI in the treatment of non-small cell lung cancer. *Clin Transl Oncol*. 2019;21(10):1287–1301. doi:10.1007/s12094-019-02075-1
30. Shi MJ, Dong BS, Yang WN, Su SB, Zhang H. Preventive and therapeutic role of Tanshinone A in hepatology. *Biomed Pharmacother*. 2019;112:108676. doi:10.1016/j.biopha.2019.108676
31. Zhou ZY, Zhao WR, Zhang J, Chen XL, Tang JY. Sodium tanshinone IIA sulfonate: a review of pharmacological activity and pharmacokinetics. *Biomed Pharmacother*. 2019;118:109362. doi:10.1016/j.biopha.2019.109362
32. Liao XZ, Gao Y, Huang S, et al. Tanshinone IIA combined with cisplatin synergistically inhibits non-small-cell lung cancer in vitro and in vivo via down-regulating the phosphatidylinositol 3-kinase/Akt signalling pathway. *Phytother Res*. 2019;33(9):2298–2309. doi:10.1002/ptr.6392
33. Zhang J, Wang J, Jiang JY, Liu SD, Fu K, Liu HY. Tanshinone IIA induces cytochrome c-mediated caspase cascade apoptosis in A549 human lung cancer cells via the JNK pathway. *Int J Oncol*. 2014;45(2):683–690. doi:10.3892/ijo.2014.2471
34. Shi P, Oh YT, Deng L, et al. Overcoming acquired resistance to AZD9291, a third-generation EGFR inhibitor, through modulation of MEK/ERK-dependent bim and Mcl-1 degradation. *Clin Cancer Res*. 2017;23(21):6567–6579. doi:10.1158/1078-0432.CCR-17-1574
35. Ye M, Zhang Y, Zhang X, et al. Targeting FBW7 as a strategy to overcome resistance to targeted therapy in non-small cell lung cancer. *Cancer Res*. 2017;77(13):3527–3539. doi:10.1158/0008-5472.CAN-16-3470
36. Arai S, Jonas O, Whitman MA, Corey E, Balk SP, Chen S. Tyrosine kinase inhibitors increase MCL1 degradation and in combination with BCLXL/BCL2 inhibitors drive prostate cancer apoptosis. *Clin Cancer Res*. 2018;24(21):5458–5470. doi:10.1158/1078-0432.CCR-18-0549
37. Nalluri S, Peirce SK, Tanos R, et al. EGFR signaling defines Mcl(-)1 survival dependency in neuroblastoma. *Cancer Biol Ther*. 2015;16(2):276–286. doi:10.1080/15384047.2014.1002333
38. Tong J, Tan S, Zou F, Yu J, Zhang L. FBW7 mutations mediate resistance of colorectal cancer to targeted therapies by blocking Mcl-1 degradation. *Oncogene*. 2017;36(6):787–796. doi:10.1038/onc.2016.247
39. Ding Q, He X, Hsu JM, et al. Degradation of Mcl-1 by beta-TrCP mediates glycogen synthase kinase 3-induced tumor suppression and chemosensitization. *Mol Cell Biol*. 2007;27(11):4006–4017. doi:10.1128/MCB.00620-06
40. Trivigno D, Essmann F, Huber SM, Rudner J. Deubiquitinase USP9x confers radioresistance through stabilization of Mcl-1. *Neoplasia*. 2012;14(10):893–904. doi:10.1593/neo.12598
41. Zhang S, Zhang M, Jing Y, et al. Deubiquitinase USP13 dictates MCL1 stability and sensitivity to BH3 mimetic inhibitors. *Nat Commun*. 2018;9(1):215. doi:10.1038/s41467-017-02693-9

**OncoTargets and Therapy**

Dovepress

**Publish your work in this journal**

OncoTargets and Therapy is an international, peer-reviewed, open access journal focusing on the pathological basis of all cancers, potential targets for therapy and treatment protocols employed to improve the management of cancer patients. The journal also focuses on the impact of management programs and new therapeutic

agents and protocols on patient perspectives such as quality of life, adherence and satisfaction. The manuscript management system is completely online and includes a very quick and fair peer-review system, which is all easy to use. Visit <http://www.dovepress.com/testimonials.php> to read real quotes from published authors.

Submit your manuscript here: <https://www.dovepress.com/oncotargets-and-therapy-journal>